5th International Conference on Experimental Fluid Mechanics – ICEFM 2018 Munich
Munich, Germany, July 2-4, 2018

Enhancement of aerodynamic performance of a wing model using an array of slotted synthetic jets

Pramod Salunkhe[1], Hui Tang[2]*,Yanhua Wu[3]

[1]Department of Mechanical Engineering, Dr. D.Y. Patil Institute of Engineering, Management & Research, Pune, Maharashtra, India

[2]Department of Mechanical Engineering, Hong Kong Polytechnic University, Hong Kong, China

[3]School of Mechanical & Aerospace Engineering, Nanyang Technological University, Singapore

*h.tang@polyu.edu.hk

Abstract

The present work deals with the improvement in aerodynamic performance of a wing model, NACA 0025, using an array of slotted synthetic jets. A new synthetic jet actuator was designed and located at 30% of the chord. Force balance and hot-wire measurements were carried out in a subsonic wind tunnel to assess the performance enhancement due to the operation of the synthetic jet array. Initially, the synthetic jet velocity was measured under quiescent flow condition at different actuation frequencies and input power. Actuation at 1000 Hz and 200 V resulted in the highest blowing velocity of 10.5 m/s. Experiments were performed at various actuation frequencies, namely, 200 HZ, 600 Hz and 1000 Hz. It was observed that, actuation at 1000 Hz led to increase in lift coefficient by 35.6% and reduction in drag coefficient by 33%. Subsequently, hot-wire measured power spectrum was computed from 40% to 80% of the chord. The power spectra showed successful stabilization of the flow field at the actuation of 1000 Hz.

1 Introduction

Active flow control over a wing model is still a hot topic of research from past few decades. One of the promising means of active flow control method is synthetic jet (SJ) technology. The transverse oscillation of piezoelectric diaphragm causes successive suction and blowing at the actuator orifice that form a train of vortex rings propagating away. The train of these vortices is called as a synthetic jet. Although its effect is local, SJ plays a key role in altering the global flow field positively. This causes the virtual modification of aerodynamic shape of the wing model.

Tang et al. (2014) described three mechanisms of SJ-based flow control over a wing model, viz. (i) direct momentum addition to the free-stream flow by blowing; (ii) momentum exchange from free-stream flow to the retarding boundary layer flow due to SJ vortex structures; and (iii) oscillation of piezoelectric diaphragm in a certain frequency range that affects the instability of shear layer. Amitay et al. (2001) reported that the best control effects can be obtained if the SJ actuators are placed close to the separation point. The lift and drag coefficients were significantly improved up to 100% and 45%, respectively at a chord Reynolds number of 7.25×10^5. When the SJ operation frequency $F^+ > 4$, the lift to pressure drag ratio was found to be reduced, whereas, when $F^+ \geq 10$, this ratio was significantly increased. Glezer et al. (2005) investigated the effects of low and high frequency actuation on an unconventional airfoil. It was reported that the high frequency actuation leads to a thin and stable boundary layer that help improve the flow-field. The low frequency actuation found to be less effective as it gives a strong coupling between the actuation frequency and the global instabilities. This coupling was not observed at high actuation frequency. In contrast to the above findings, Frank and Colonius (2012) in their computational investigations reported that the low frequency actuation in the order of natural shedding frequency is the most effective in decreasing the separation region as compared to high frequency actuation. This was

attributed to the formation of large vortical structures that help re-attach the flow. The high frequency actuation forms small vortices that dissipate rapidly. Timor et al. (2007) carried out experimental studies on NACA 0018 airfoil over a range of Re = 1.6×10^5 to 3×10^5 using an array of 14 SJ actuators placed at 88% of the chord. The lift coefficient was found to be significantly increased after switching on all the actuators. The rolling moment was found to be substantially increased when only the half-span of the wing was actuated with the SJ array. Sefcovic and Smith (2010) located an array of SJ actuators at the leading and trailing edge of NACA 65_2 -215 airfoil. It was observed that the leading-edge actuators help control flow separation and increase the maximum lift coefficient. The trailing-edge actuators were found to enhance the lift-to-drag ratio below the stall angle of attack.

Salunkhe et al (2016) analyzed the effectiveness of SJ arrays on an airfoil LS(1)-0421MOD using tomographic PIV measurements. The highest effectiveness of the actuators was observed at 180^o phase angle which corresponds to the instant when the maximum blowing occurs. The improvement in wing performance due to the SJ arrays was attributed to the exchange of momentum between the secondary vortices propagating downstream and the retarding boundary layer flow. Rimasauskiene et al. (2015) optimized the design of a SJ actuator for the highest possible SJ velocity. The parametric study was carried out by varying the number of orifices and cavity height. The highest SJ velocity of 25 m/s was obtained for the configuration of single orifice and cavity height of 0.5 mm.

Following our previous work (Tang et al. 2014), the aim of the present work is to design a new SJ array with a reduced number of piezoelectric diaphragms that can impart higher momentum as compared to our previous SJ arrays. Reduction in number of piezoelectric diaphragms substantially reduces the power consumption. Other objective of the present work is to estimate the performance improvement of the wing by varying the SJ actuation frequency. The wing performance is assessed through different parameters, namely, lift coefficient, drag coefficient and FFT power spectra.

2 Experimental Set-up and Instrumentation

Experiments were carried out in a subsonic wind tunnel of size 2 m × 0.78 m × 0.72 m on NACA 0025 airfoil with a realistic free-stream flow speed of 10 m/s. This flow speed corresponds to a Reynold number of 1.5×10^5. The wing has a chord of 0.24 m and span of 0.4 m. A new SJ actuator was designed as depicted in Fig. 1(a). It comprises of two piezoelectric diaphragms separated by a cavity height of 8 mm. It generates SJ through a rectangular slot of 0.5 mm (W) × 12 mm (L) × 2 mm (H) that is cut on the suction surface of the NACA 0025 wing model. Eleven such actuators were installed inside the wing model at 30% of the chord and evenly distributed in the spanwise direction, as shown in Fig. 1(b). In the present work, in total twenty-two piezoelectric diaphragms were used as against forty diaphragms in our previous work (Tang et al., 2014). The center-to-center distance between the two successive SJ slots is 35 mm. The SJ array was driven in phase using two power amplifiers (EPA-104 from Piezo Systems Inc., USA). A function generator was used to generate a sinusoidal waveform at different frequencies.

A six-component force balance system was used to measure the axial and normal forces acting on the wing. These forces were further resolved to obtain the lift and drag forces. A hot-wire anemometer (Miniature CTA 54T30 from Dantec Dynamics A/S, Denmark) with one-dimensional hot-wire probe, 55P16, was used to measure the jet velocity generated by the actuators. The probe has a 5 μm diameter and 1.25 mm long platinum-plated tungsten wire sensor. The sampling frequency and number of samples were set to 10 kHz and 1000, respectively.

Uncertainty in the velocity measurement using the hot-wire probe was about 0.8%, whereas, uncertainty in lift and drag measurements were 0.2% and 0.5%, respectively.

3 Results and Discussion

The SJ array was driven at 200 V peak voltage at various frequencies, namely, 200 Hz, 600 Hz and 1000 Hz. The corresponding reduced frequencies, defined as $F+ = fc/U_\infty$, were 4.8, 14.4 and 24, respectively. The strength of a vortex is determined from the Stokes number which is the ratio of unsteady force to the

viscous force. The vortex ring rolls up if the Stokes number is higher than 10 (Zhou et al. 2009). The Stokes number at 200 Hz, 600 Hz and 1000 Hz was found to be 7.5, 15.2 and 19.6, respectively. The momentum coefficient represents the momentum transferred by the SJ actuators to the boundary layer flow. It was determined from the equation, $C_\mu = nAU_j^2/bcU_\infty^2$. The momentum coefficients for the SJ actuation at 200 Hz, 600 Hz and 1000 Hz were found to be 2.4×10^{-6}, 1.6×10^{-4} and 7.8×10^{-4}, respectively.

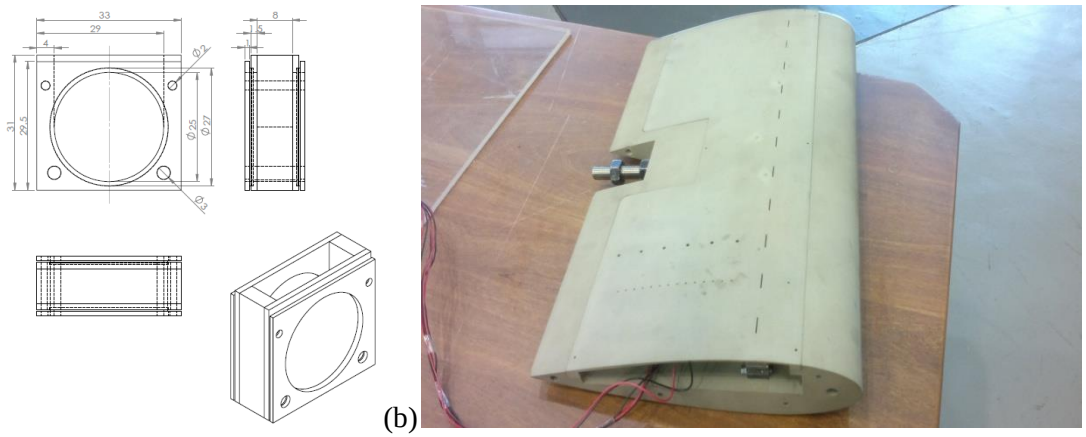

(a) (b)

Figure 1: (a) SJ actuator geometry and (b) pictorial view of the NACA 0025 wing model with the SJ array

The SJ velocity at the exit plane of actuator slot was determined using a hot-wire probe. The probe was placed at the slot center aligned with the axis of the slot. Figure 2 represents the variation in SJ velocity against different excitation voltages, namely, 100 V, 150 V and 200 V. It can be seen that, for a given excitation voltage, the SJ velocity increases with the increase in frequency. For all the cases, it reaches a peak at 1 kHz and drops beyond that. Amongst all the excitation voltages, the highest SJ velocity of 10.5 m/s occurred at 200 V. The present piezoelectric diaphragm's resonance frequency is 4.6 kHz. This resonance frequency is significantly higher than the 1 kHz frequency, which indicates that the 1 kHz frequency is the Helmholtz frequency of the SJ actuator. It is also observed that beyond the Helmholtz frequency, the SJ velocity drops gently for the 100 V and 150 V excitation, whereas, it drops abruptly for 200 V excitation.

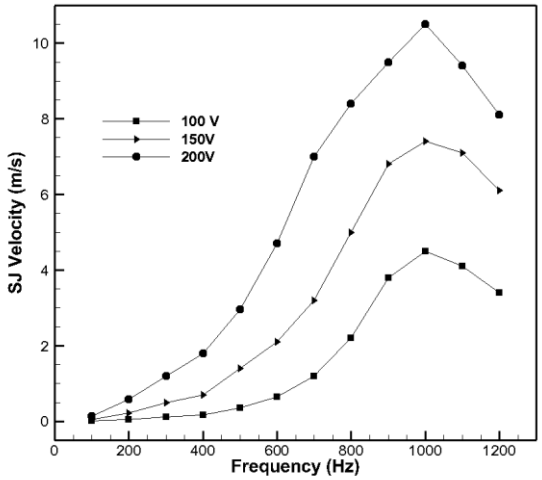

Figure 2: Variation of SJ velocity against actuation frequencies

The force balance measurements were carried out to determine the lift and drag coefficients. Figure 3(a) shows the variation in the lift coefficient against various angles of attack (AOA) for different SJ actuation

frequencies. It is observed that up to 10^o AOA, the variation in lift coefficient is marginal for both the baseline and actuated cases. For the baseline case, the lift coefficient increases gradually up to 18^o AOA, and then drops abruptly representing the onset of stall. The SJ actuation at 600 Hz shows the onset of stall after 20^o AOA. In addition, the reduction in lift coefficient is very mild between 20^o to 24^o AOA. The gentle reduction in lift coefficient is attributed to the increased resistance to the flow separation due to increase in momentum coefficient corresponding to the actuation at 600 Hz. Beyond 24^o AOA, the increased pressure gradient prevails the resistance to flow separation and causes a sharp reduction in lift coefficient. Surprisingly, after switching on the SJ array at a frequency of 1000 Hz, the lift coefficient is gradually increased and has not entered the stall mode of operation in the investigated frequency range. This shows that the actuation at 1000 Hz is significantly effective for the flow separation control. The enhancement in lift coefficient for the 200 Hz, 600 Hz and 1000 Hz over the baseline case was found to be 1.7%, 20.5% and 35.6%, respectively. The highest improvement at 1000 Hz can be attributed to the higher Stokes number of 19.6 and higher SJ velocity of 10.5 m/s which results in high momentum coefficient of 7.8×10^{-4}. The higher Stokes number leads to the high vortex strength and deeper penetration of the SJ into the primary flow resulting in higher momentum transfer and hence improvement in wing performance. Amongst all actuation cases, the SJ actuation at 200 Hz resulted in negligible improvement in lift coefficient. As the SJ actuation at 200 Hz results in a significantly low momentum coefficient of 2.4×10^{-6} and Stokes number of only 7.5, the jet strength is not enough to penetrate the primary flow and supply the much needed momentum to the boundary layer flow.

Figure 3(b) shows the variation in drag coefficient against various AOAs at different SJ frequencies. It is observed that for the baseline case, the drag coefficient increases steadily until 18^o AOA. After the onset of flow separation, the drag coefficient shoots up abruptly due to the sharp rise in pressure drag. Among all the cases, the largest reduction in average drag coefficient of 33% is observed for the actuation at 1000 Hz as the wing has not experienced the onset of stall in the investigated frequency range. The actuation at 600 Hz resulted in the reduction of average drag coefficient by 25%, whereas, actuation at 200 Hz was found to be negligible in terms of reduction in average drag coefficient.

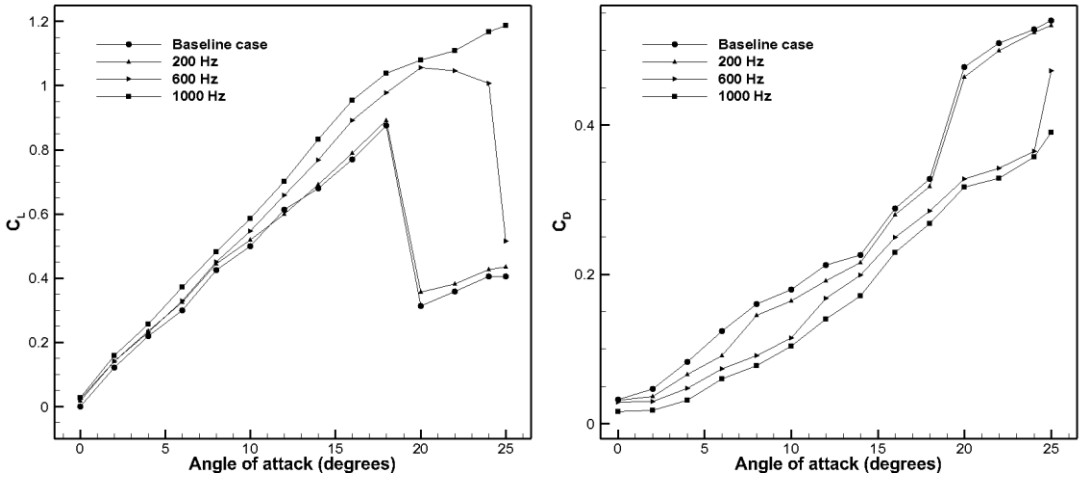

Figure 3: Variation in (a) lift coefficient and (b) drag coefficient against angles of attack

Fast Fourier Transform (FFT) power spectrum was computed based on the hot-wire measurements. The wing was set at 18^o AOA. The hot-wire probe was placed 8 mm above the suction surface and traversed from 40% to 80% of the chord with a uniform spacing of 8% of the chord. The FFT power spectrum

shows the variation in power of a given signal against different frequencies. The power of a signal shoots up after the occurrence of a disturbance or stall precursor. In order to prevent or delay the onset of flow separation, damping of these flow disturbances is very important. Figure 6 shows the FFT power spectrum for the baseline and various SJ actuation cases. Figures 4(a)-4(c) show a spike in the SJ actuated case which corresponds to the actuation frequency. This spike was not observed when the hot-wire probe was traversed beyond 56% of the chord as the probe location is far away from the SJ location to detect the actuator frequency. It was observed that the SJ actuation at 600 Hz and 1000 Hz are significantly effective in damping out the disturbances. Figure 4(a) shows that up to 1000 Hz frequency, the mean FFT power spectrum for the baseline case lies in the range of -5 dB to -30 dB. It reduced in the range of -30 dB to -40 dB for the actuation at 1000 Hz. It was also found that the effectiveness of the SJ actuation reduces from the leading edge towards the trailing edge as can be seen in subplots Fig. 4(a)-4(f). Actuation at 200 Hz was found to be ineffective as compared to other actuation cases. The above results indicate that the present SJ array is very effective in stabilizing the flow field at the actuation frequencies of 600 Hz and1000 Hz. It is anticipated that the stabilization of flow field is associated with reduction in the strength of the flow structures that are evolved due to the flow separation. The effectiveness of the SJ array at the actuation frequencies of 600 Hz and 1000 Hz is also supported by the force balance measurements as seen in Fig. 3.

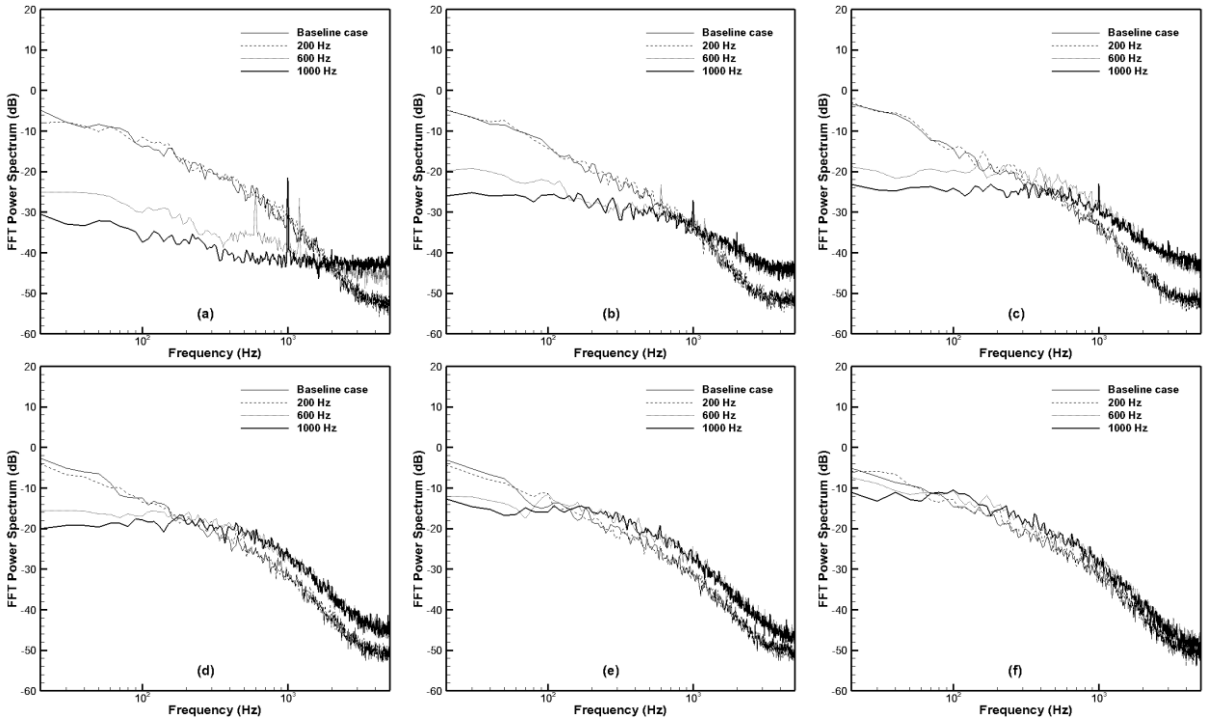

Figure 4: FFT power spectra for the baseline case and the actuation cases at different frequencies along (a) 40% (b) 48% (c) 56% (d) 64% (e) 72% and (f) 80% of the chord

The above results are in-line with our previous works (Tang et al. 2014; Salunkhe et al. 2016), wherein, the highest performance improvement was observed at the SJ actuator's Helmholtz frequency. The PIV measurements demonstrated that the introduction of SJ significantly reduces the strength of uncontrolled large-scale flow structures associated with the flow separation and enhances the momentum of the boundary layer flow. In the present work, it is anticipated that the similar mechanism is responsible for the performance enhancement for the actuation at 1000 Hz.

4 Conclusions

Experiments were carried out in a subsonic wind-tunnel on an airfoil NACA 0025 with a SJ array installed. The SJ array was operated at various actuation frequencies of 200 Hz, 600 Hz and 1000 Hz. The highest wing aerodynamic performance was observed at an actuation of 1000 Hz, with 35.6% enhancement in lift coefficient and 33% reduction in average drag coefficient. The FFT power spectrum showed the substantial reduction in the power spectrum for the actuation at 1000 Hz leading to successful stabilization of the flow field. The SJ array was found to be more effective at the leading edge than at the trailing edge. Both the force-balance and hot-wire results showed that the actuation at 200 Hz results in negligible performance improvement. The highest performance improvement at an actuation of 1000 Hz can be attributed to the substantially high momentum coefficient of 7.8×10^{-4} and high Stokes number of 19.6 that help impart more momentum to the retarding boundary layer flow. A thorough analysis of the flow dynamics of flow separation and reattachment will be the future scope of the present work.

References

Amitay A, Smith DR, Kibens V, Parekh DE and Glezer A (2001) Aerodynamic flow control over an unconventional airfoil using synthetic jet actuators. *AIAA Journal* 39:361-370

Franck JA and Colonius T (2012) Effects of actuation frequency on flow control applied to a wall-mounted hump. Technical Note. *AIAA Journal* 50:1631-1634

Glezer A, Amitay M and Honohan AM (2005) Aspects of low- and high-frequency actuation for aerodynamic flow control. *AIAA Journal* 43:1501-1514

Rimasauskiene R, Matejka M, Ostachowicz W, Kurowski M, Malinowski P, Wandowski T, Rimasauskas M (2015) Experimental research of the synthetic jet generator designs based on actuation of diaphragm with piezoelectric actuator. *Mechanical Systems and Signal Processing* 50-51:607-614

Salunkhe PB, Tang H, Zheng Y and Wu Y (2016) PIV measurement of mildly controlled flow over a straight-wing model. *International Journal of Heat and Fluid Flow* 62:552-559

Sefcovic JA and Smith DR. Proportional aerodynamic control of a swept divergent trailing edge wing using synthetic jets. *48th AIAA Aerospace Sciences Meeting*, 4^{th} – 7^{th}Jan. 2010, Orlando, Florida

Tang H, Salunkhe PB, Zheng Y, Du J and Wu Y (2014) On the use of synthetic jet actuator arrays for active flow separation control. *Experimental Thermal and Fluid Science*57:1-10

Timor I, Hamou EB, Guy Y and Seifert (2007) Maneuvering aspects and 3D effects of active airfoil flow control. *Flow Turbulence Combust* 78:429-443

Zhou J, Tang H, Zhong S (2009) Vortex roll-up criterion for synthetic jets. *AIAA Journal* 47:1252–1262.